

Review

# Three-Dimensional Printing, an Emerging Advanced Technique in Electrochemical Energy Storage and Conversion

Shu Zhang <sup>1,2</sup>, Shuyue Xue <sup>1</sup>, Yaohui Wang <sup>1</sup>, Gufei Zhang <sup>3</sup>, Nayab Arif <sup>2</sup>, Peng Li <sup>1,\*</sup> and Yu-Jia Zeng <sup>2,\*</sup> <sup>1</sup> Department of Chemical Engineering, Shandong University of Technology, Zibo 255000, China<sup>2</sup> Key Laboratory of Optoelectronic Devices and Systems of Ministry of Education and Guangdong Province, College of Physics and Optoelectronic Engineering, Shenzhen University, Shenzhen 518060, China; nayabarif@szu.edu.cn<sup>3</sup> POLIMA-Center for Polariton-Driven Light-Matter Interactions & Danish Institute for Advanced Study, University of Southern Denmark, Campusvej 55, DK-5230 Odense M, Denmark; gufei@mci.sdu.dk

\* Correspondence: szplapc@sdu.edu.cn (P.L.); yjzeng@szu.edu.cn (Y.-J.Z.)

**Abstract:** Three-dimensional (3D) printing, as an advanced additive manufacturing technique, is emerging as a promising material-processing approach in the electrical energy storage and conversion field, e.g., electrocatalysis, secondary batteries and supercapacitors. Compared to traditional manufacturing techniques, 3D printing allows for more precise control of electrochemical energy storage behaviors in delicately printed structures and reasonably designed porosity. Through 3D printing, it is possible to deeply analyze charge migration and catalytic behavior in electrocatalysis, enhance the energy density, cycle stability and safety of battery components, and revolutionize the way we design high-performance supercapacitors. Over the past few years, a significant amount of work has been completed on 3D printing to explore various high-performance energy-related materials. Although impressive strides have been made, challenges still exist and need to be overcome in order to meet the ever-increasing demand. In this review, the recent research progress and applications of 3D-printed electrocatalysis materials, battery components and supercapacitors are systematically presented. Perspectives on the prospects for this exciting field are also proposed with applicable discussion and analysis.



**Citation:** Zhang, S.; Xue, S.; Wang, Y.; Zhang, G.; Arif, N.; Li, P.; Zeng, Y.-J. Three-Dimensional Printing, an Emerging Advanced Technique in Electrochemical Energy Storage and Conversion. *Batteries* **2023**, *9*, 546.

<https://doi.org/10.3390/batteries9110546>

Academic Editor: Changshin Jo

Received: 4 September 2023

Revised: 8 October 2023

Accepted: 12 October 2023

Published: 6 November 2023



**Copyright:** © 2023 by the authors. Licensee MDPI, Basel, Switzerland. This article is an open access article distributed under the terms and conditions of the Creative Commons Attribution (CC BY) license (<https://creativecommons.org/licenses/by/4.0/>).

## 1. Introduction

After the first, second and third industrial revolutions driven by steam power, electricity, and information technology, respectively, the world is experiencing the fourth industrial revolution, with additive manufacturing as one of the fascinating driving forces [1]. Additive manufacturing, also termed as “three-dimensional (3D) printing”, is a cutting-edge technology that integrates materials science, electrical control technology, digital technology, information science technology and many other fields [2,3]. Developed in the 1980s, it aims to meet the needs of model production and rapid prototyping. Nowadays, it has grown into a multi-functional technology platform involving structural design and manufacturing. Up to now, several methods for the construction of organized battery structures, such as photo etching, have been developed and improved; by means of photosensitive materials and chemical agents, the desired patterns can be obtained through rational photo etching process [4]. In comparison, 3D printing technology has better design freedom, and it significantly changes people’s cognition of product design, manufacturing and use [5–7]. Additive manufacturing pertains to an industrial method of production; it creates objects via layer-by-layer printing using metal or plastic powder based on a specific digital model file during the fabrication process [8]. In accordance with the manner in which the 3D architecture is produced, the printing process can be mainly classified as extrusion printing, inkjet printing, powder bed fusion printing, adhesive jet printing, directed

energy fusion printing or reduction photopolymerization printing [9]. These emerging 3D printing techniques allow for a vast assortment of functional structures with highly programmable structural features. This is difficult to accomplish through conventional approaches. Therefore, these technologies open up new pathways for constructing advanced energy storage device.

Firstly, a 3D model with three-dimensional data in the virtual 3D space on the basis of the target object is created. Generally, some models can be directly downloaded from professional websites, and 3D scanners can also be utilized for reverse engineering modeling, during which 3D data models could be obtained through scanning real-world objects. In addition, some software, such as SolidWorks, AutoCAD and Blender, can be utilized to directionally design specific models. Then, the model is sliced into plenty of two-dimensional cross sections. After selecting suitable printing precursors and setting up accurate parameters, the 3D printer can finish layer-by-layer material printing successively [10,11]. Notably, a stable work platform, appropriate temperature and precisely controlled humidity are required during the printing process. Due to its features in preparing structural objects layer by layer, the thickness of the manufactured electrode can be effectively regulated. In addition, the periodic or specific regular spatial structure of the cavity in the battery can comprehend the rapid ion transportation. Under the 3D printing manufacturing process, the region where the electrode and the electrolyte come into contact grows, which guarantees this technology's promising application [12,13]. Lately, a considerable amount of work has been conducted within the field of 3D printing for electrochemical energy-storage (batteries and supercapacitors) and -conversion (electrocatalysis) applications [14,15]. For electrocatalysis, 3D printing is a promising approach for improving the efficiency of electrocatalysis processes. The excellent flexibility and stability of graphene and carbon nanotubes make them highly suitable for 3D printing. However, at present, only a limited number of optimization methods can be employed in this technology to effectively enhance the electrocatalytic performance of products, such as O<sub>2</sub> plasma treatment and hydrothermal immersion. In terms of battery construction, the application of 3D printing technology in battery component production, including positive and negative electrodes, electrolytes, and separators, can lead to remarkable results. Notably, printed components with a rational design and microstructure could provide excellent electrochemical performance in batteries. In printed supercapacitors, 3D printing technology is capable of creating almost any desired shape, eliminating the need for molds or photomasks. This feature allows for adjustable geometry, high integration, time and cost savings, as well as superior power and energy density. Although the conventional blade-casting method is better than 3D printing in terms of utilization efficiency at this stage, 3D printing still shows substantial advantages regarding design freedom, low complexity, device miniaturization and high accuracy. Furthermore, the additive nature and precise ink deposition process significantly enhances the material utilization ratio and minimizes wasteful depletion, which aligns with the developing trend of sustainable storage device. Especially in recent years, portable wearable electronic devices have attracted more and more attention, triggering significant demand for battery shape freedom [9,16]; 3D printing technology is considered to be one of the most promising keys to this. Moreover, conductive devices can be produced easily via this technique. During electrochemical reactions, the application of nanomaterials with a large specific surface area has a great prospect advantage [17]. With the support of 3D printing technology, the obtained nanostructure can provide good activity for electrochemical reactions [18].

In this review, the recent advances in 3D printing in the electrical energy storage and conversion field are systematically presented. Followed by the insights generated by the review of typical works, a brief summary and analysis of the challenges and trends for next-stage investigation and development are further proposed.

## 2. Electrocatalysis

Nowadays, global warming and fossil energy consumption have attracted enormous attention worldwide, and green energy technologies are receiving a lot of attention, including electrocatalytic reactions and gas–liquid–solid interfacial catalysis [19,20]. Although high catalyst loading leads to more exposed active sites, the diffusion rate of electrons and reactants in the thick catalyst layer may be reduced, and thus mass transfer in the electrode becomes more difficult, resulting in the degradation of catalytic activity. In order to further enhance the effectiveness of the three-phase interfacial electrocatalytic reaction, it is necessary to explore a reliable three-dimensional electrode/support in which the charge migration and catalytic behavior should be deeply analyzed [21]. Three-dimensional printing can produce a complex architecture in one step without any additional processing. Note that 3D-printed products demonstrate satisfactory compression resistance, elasticity and stiffness, as the multilayer 2D graphene nanosheets could act as effective mutual support under compressive stress. Recently, graphene electrodes with reliable mechanical strength prepared via a 3D printing strategy illustrated great potential in advanced energy, environmental fields, electronic systems and other fields. Graphene is an appealing choice for electrocatalytic applications due to its 2D hexagonal honeycomb structure, which is formed by strong sp<sub>2</sub> hybridized carbon–carbon bonds and exhibits exceptionally high heat conductivity and excellent electrical conductivity. To promote the porosity development with a high surface area and ideal strength, Jiang and his coworkers prepared a kind of 3D-printed bioinspired electrode in which the graphene matrix was strengthened with 1D carbon nanotubes (CNTs) (3DP GC). Then, through a extrusion-based printing approach using a partially reduced graphene oxide (pr-GO)/CNT mixed ink, a hierarchical porous structure was finally built [22]. As illustrated in Figure 1a, 3DP G electrodes had a microscopic porosity which resembled that of 3DP GC electrodes (Figure 1c). The walls of 3DP G electrodes were composed of multilayer graphene (Figure 1b), while graphene/interlaced CNTs comprised those of 3DP GC (Figure 1d). The CNTs in the 3DP GC electrode remarkably promotes the friction between graphene nanosheets, leading to high biomimetic mechanical property and optimized tensile strength of the graphene/interlaced CNT wall. The 3D-printed electrode (3DP GC) combining 1D CNT and 3D graphene was further treated with O<sub>2</sub> plasma for 5 min, and then hydrothermally immersed in an aqueous solution containing NH<sub>4</sub>F, urea, NiCl<sub>2</sub> and FeCl<sub>3</sub> for 15 h. After calcination in Ar together with NaH<sub>2</sub>PO<sub>2</sub> at 350 °C, a NiFeP catalyst could be obtained. In addition, carbon paper/NiFeP and nickel foam/NiFeP electrodes were also synthesized and adopted as references in HER and OER reactions. After the 3D-printed electrode was loaded with a NiFeP nanosheet, a current density of 30 mA cm<sup>-2</sup> was achieved at a voltage of 1.58 V during the water splitting process, much higher than previously proposed Ni-, Co-, and Fe-based electrocatalysts. It can be concluded that the desirable intrinsic conductivity and developed porosity of the 3DP GC/NiFeP electrode triggers applicable electron, ion and gas transport in HER and OER (Figure 1e), and this approach demonstrates remarkable potential in energy storage and conversion. Generally, the exploitation of 3D supports with desirable efficiency for electrocatalytic reactions at the gas–liquid–solid interfaces is vital for decreasing energy loss. Considering that it is highly difficult to prepare geometrically complex 3D supports directly using conventional methods, Ding et al. developed a tough catalyst support with a tailored 3D architecture through facile printing [23]. SolidWorks2012 3D modeling software was first used to design the specific structures of supports, and then spherical 316L stainless steel powder (30 µm, average particle size) was applied to prepare stainless steel electrodes. Metal printing was implemented through SLM equipped with a ytterbium fiber laser under inert atmosphere. A Teflon-lined stainless-steel autoclave filled with 10 mM cobalt nitrate, 5 mM nickel nitrate and 15 mM urea was heated and maintained for 10 h, during which the catalyst could grow on the clean and conductive stainless steel support. As can be seen, NiCo<sub>2</sub>S<sub>4</sub> nanoneedles were uniformly loaded on the 3D-printed support with large holes (Figure 1f), and the vertical needles exhibited homogeneous Ni, Co, and S distribution (Figure 1g). Notably, excellent electrochemical properties were provided. When tested at

high current density ( $100 \text{ mA cm}^{-2}$ ), the obtained electrode demonstrated a low overpotential (277 mV). This kind of work demonstrates the progress made in the 3D printing of metal using SLM technology, allowing the creation of next-generation electrocatalytic supports for diverse electrochemical applications. In addition, this work, integrating 3D printing and wet-chemical nanotechnology, realized an impressive 3D-printed electrocatalyst over the size scale from macro (steel substrate) to micro (micro-holes and micro pores) and nano (nanoneedles). Furthermore, Martin and coworkers coated ZIF-67 onto the surface of 3D-printed titanium electrodes using step-by-step in situ growth and then converted it into cobalt oxide by means of electrochemical cycling. This large-surface-area  $\text{Co}_3\text{O}_4$ , as well as the existence of  $\text{Co}^{\text{IV}}$  species right before water oxidation, plays a critical role in enhanced electrocatalytic performance under alkaline electrolysis conditions with a low overpotential of 360 mV at a current density of  $10 \text{ mA cm}^{-2}$  and excellent durability [24]. Using a similar coating method, they modified the 3D-printed electrode surface with highly catalytic  $\text{MoS}_x$ . The scanning electron microscopy revealed the heterogenous behavior of the catalyst, providing valuable insights into its performance at a larger scale [25]; this paves the way for enhancing the catalyst material and the development of effective electrochemical devices with related typical research works organized in Table S1 [22–26]. To sum up, utilizing 3D printing technology, it is possible to deeply analyze charge migration and catalytic behavior, and ultimately leads to improved electrocatalysis performance. The use of 3D printing to produce complex architectures without additional processing makes it a promising approach for the development of advanced energy-related systems; it can significantly enhance the efficiency and flexibility of the preparation methods in the field of electrocatalysis. Moreover, it opens up a plethora of possibilities for the application of electrocatalysis.

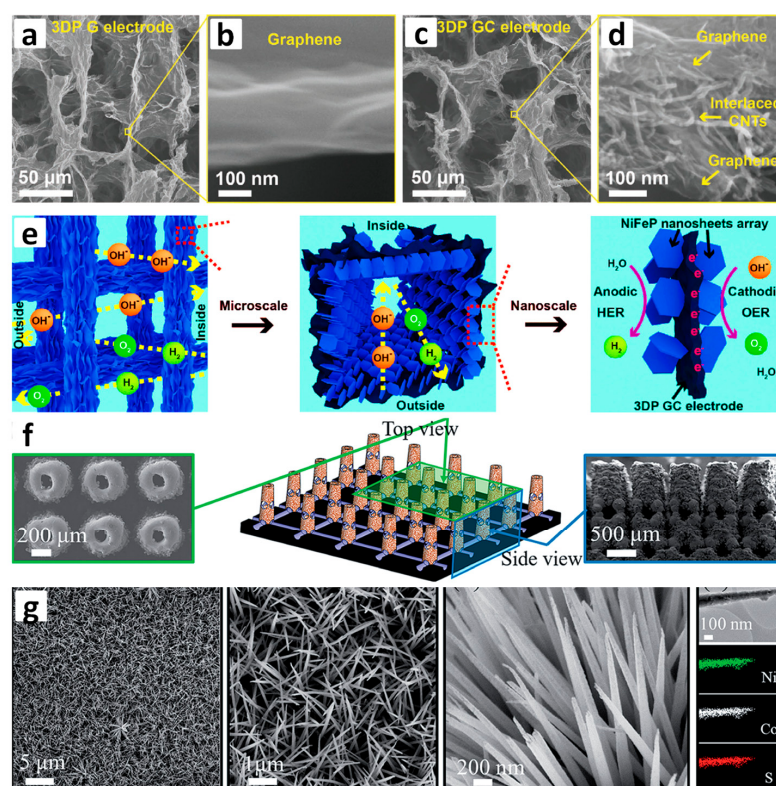


**Figure 1.** (a–d) SEM images of a 3D-printed bioinspired electrode of graphene reinforced with 1D carbon nanotubes (3DP GC). (e) Schematic diagram of the hierarchical porous structure of 3DP GC/NiFeP electrode-facilitated ion and gas transport for both the anode (HER) and cathode (OER) of water splitting. Reproduced with permission [22]. Copyright 2020, Wiley. (f) SEM images of a 3D-printed hierarchical support with hollow porous cone arrays. (g) High-magnification SEM images of  $\text{NiCo}_2\text{S}_4$  nanoneedles on the side of porous cones and corresponding elemental mapping images. Reproduced with permission [23]. Copyright 2020, Wiley.

### 3. Secondary Battery

Energy storage secondary batteries are increasingly important for portable electronic devices [27]. The demand for batteries with a unique structure and optimized energy storage capacities in mobile electronic devices is also increasing. At present, most batteries are cylindrical or rectangular, greatly limiting the size and shape of mobile electronic devices [28]. The use of 3D printing provides significant advantages for their rapid prototyping of special structures; it can reasonably meet the aforementioned development demand [29]. Generally, secondary batteries mainly contain three parts, i.e., a cathode, anode and electrolyte. Up to now, researchers have made great advances in these three aspects.

#### 3.1. Three-Dimensionally Printed Cathode

The problem in producing cathodes is further complicated by the generally controlled conditions required for cathode electrode preparation, particularly moisture control. With an increase in the thickness of the electrode, the electron transmission distance and total electrical impedance of the electrode inevitably grow, leading to a decrease in power density and rate capability. As compared to the conventional two-dimensional planar design, a three-dimensional structure can produce a shorter diffusion path and lower resistance. Recently, Hu et al. reported the application of scalable, low-cost, high-efficiency 3D printing technology in the fabrication of a lithium iron phosphate (LFP) cathode [30]. As shown in Figure 2a, the ink was sprayed into a coagulation bath using an air-powered fluid dispenser, and it was subsequently extruded into ethanol and encapsulated by a PVDF fibrous gel containing nanoparticles. It is impressive that this process could generate high-quality and uniform fibers in a short timeframe. An all-fiber LIB device was constructed using the printed LFP material as the cathode (Figure 2b). The charge and discharge cycles of electrodes at 50 mA g<sup>-1</sup> illustrated an initial lithiation capacity of 141.3 mAh g<sup>-1</sup>. After 30 cycles, the lithiation capacity slightly decreased to 91.7 mAh g<sup>-1</sup> and 89 mAh g<sup>-1</sup>, respectively, demonstrating an impressive capacity retention (81%). Notably, since the obtained fibers have great flexibility and reliable strength, they could also be transformed into a textile structure by weaving them together, as shown in Figure 2c, revealing that it is feasible to fabricate the printed LFP fiber into portable devices for further practical applications. Three-dimensional printing has also aroused great interest in the design of sulfur cathodes. However, previously reported printed sulfur electrodes mostly originated from carbon-based materials; electrocatalyst-loaded cathodes have not been exploited to promote sulfur redox kinetics. Liu and coworkers first prepared a mixed ink of sulfur/carbon and LaB<sub>6</sub> electrocatalysts and then developed a self-supporting sulfur cathode using 3D printing technology [31]. Interesting shapes and complicated layouts could be printed on flexible substrates, which fully demonstrated that the 3D printing process is highly versatile (Figure 2d). Moreover, through layer-by-layer printing from 1 to 10 layers, the cathode could be obtained with LaB<sub>6</sub>/SP@S-based ink. As shown in Figure 2e, the LaB<sub>6</sub> powder can sufficiently decolor the Li<sub>2</sub>S<sub>6</sub> after 6 h, revealing its good adsorption toward Li<sub>2</sub>S<sub>6</sub> and the catalytic effect of LaB<sub>6</sub> on carbon scaffold. Nevertheless, the color of Li<sub>2</sub>S<sub>6</sub> solution experienced little change with the addition of bare SP. Cyclic voltammogram profiles were also recorded in the voltage window of 1.7–2.8 V at a sweep rate of 0.05 mV s<sup>-1</sup>, in which the 3DP-LaB<sub>6</sub>/SP@S exhibited a shift to a higher potential in the cathodic sweep and a shift to a lower potential in the anodic sweep. This implies that the sulfur reaction kinetics could be promoted upon the incorporation of LaB<sub>6</sub>. Therefore, the architecture with optimized Li<sup>+</sup>/e<sup>-</sup> transmission channels and developed porosity is beneficial to efficient polysulfide management. Three-dimensionally printed structures can improve the ion/electron transfer and ultimately be beneficial to the optimization of the interfacial contact between the electrode and electrolyte ions, thus enhancing the electrochemical performance.

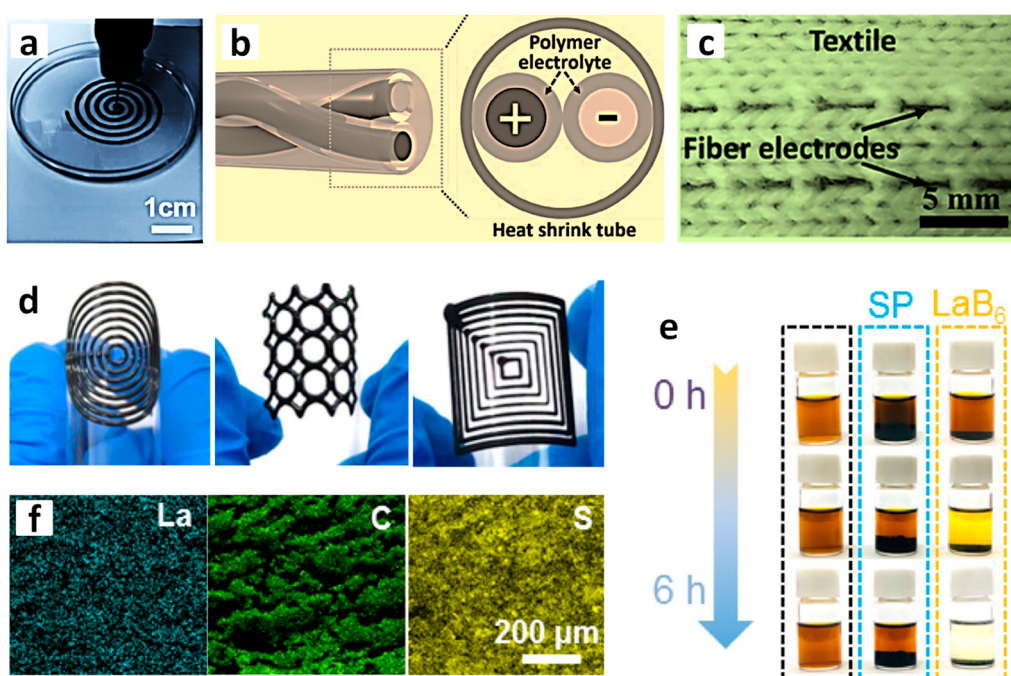


**Figure 2.** (a) The optical image of a wet fiber during the printing process. (b) Schematic of the all-fiber LIB device. (c) A photo image to demonstrate the integration of fiber electrodes into textile fabrics. Reproduced with permission [30]. Copyright 2017, Wiley. (d) Photographs of various printing patterns on PET substrate using LaB<sub>6</sub>/SP@S composite ink. (e) Visualized adsorption tests of LaB<sub>6</sub> and SP in Li<sub>2</sub>S<sub>6</sub> solution, and (f) elemental mappings of the 3DP-LaB<sub>6</sub>/SP@S. Reproduced with permission [31]. Copyright 2020, Elsevier.

### 3.2. Three-Dimensionally Printed Anode

Battery anodes, such as lithium metal, with large specific capacity, low oxidation potential, and ultrahigh energy density are expected to be the next generation of anodes for superior batteries [32,33]. However, during long cycling, lithium dendrites always come into being, which easily damage the separator film and induce harmful short circuiting, suppressing its commercialization [34,35]. Also, the change in volume of the lithium anode during charging and discharging causes a large interface resistance, which results in unsatisfactory coulombic efficiency and cycle performance. Recent studies have shown that the dendrite generation can be effectively inhibited and the volume expansion problem can be reduced by adjusting the electrode structure, electric field and the distribution of the Li-ion concentration. However, poor rate performance and low area-specific capacity are still challenges in the application of lithium metal anodes. In order to solve the aforementioned problems, Wang et al. designed and constructed a type of nitrogen-doped carbon frame electrode, taking advantage of zinc metal volatilization at high temperatures using an extrusion-based 3D printer (Figure 3a) [36]. The 3DP-Zn-MOF maintains a mesh-like structure and consists of filaments (~200 μm) stacked on top of each other with numerous large pores created (Figure 3b); after calcination, the mesh-like feature can be well maintained (Figure 3c). The 3D-printed carbon frame (3DP-NC) embraces the benefits of a hierarchical porous structure, large surface area and nitrogen-modified carbon, which are conducive to uniform lithium metal deposition and areal capacity enhancement (up to 30 mAh cm<sup>-2</sup>) (Figure 3d). At the same time, it could substantially mitigate dendrite generation, guarantee the safety of the battery system and improve the rate performance. This work combines 3D printing technology with Zn-MOF material, providing a novel technical route for heteroatom modification in carbon frameworks. In addition, unrestrained dendrite generation also reduces electrochemical properties in sodium anodes and causes safety issues, hindering the practical applications of metallic sodium anodes. To create a robust matrix for sodium plating and stripping, a 3D rGO/CNT microlattice aerogel

with a large surface area was proposed by Wang's group [37]. Gel-like GO ink was firstly obtained through dispersing 200 mg of GO into 5 mL of DI water under ultrasonication and magnetic stirring for several days, and then GO/CNT ink was obtained through adding 500 mg of hydrophilic CNTs into the prepared GO slurry. After ink was loaded into a 5 mL syringe, an air-powered dispenser was used to control the flow of GO and GO/CNT inks (Figure 3e). The rGO/CNT microlattice was finally obtained after freeze-drying for 48 h and calcination at 600 °C for 2 h; it could be utilized as the sodium metal host, taking advantage of the ordered porosity, large surface and adjustable thickness (Figure 3f). As a result, the Na@rGO/CNT microlattice anode serves an area capacity of 1 mAh cm<sup>-2</sup> and a desirable overpotential of 17.8 mV. In addition, there is an impressive cycling property (640 cycles at 8 mA cm<sup>-2</sup>), which could be attributed to the inhibited sodium metal dendrites and abundant active nucleation sites. The simulation results further verify that this good property is attributed to the optimized 3D-microstructured aerogel with tuned surface kinetics. This work shows that the rGO/CNT microlattice aerogel is a promising anode candidate as a stable sodium-metal host material for next-generation sodium-ion battery technology.

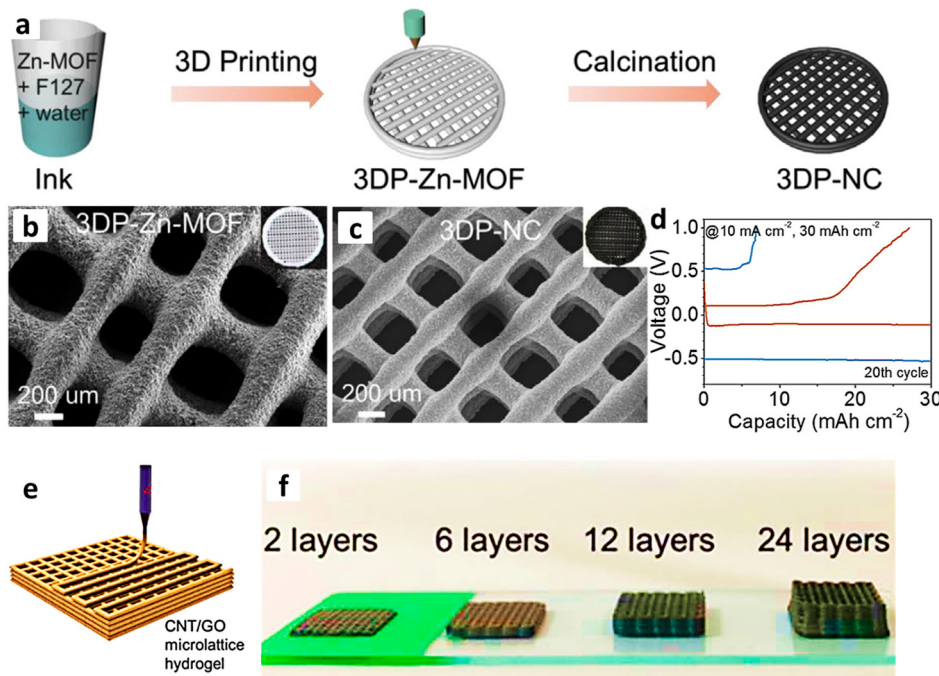


**Figure 3.** (a) Schematic of the fabrication process of 3DP-Zn-MOF and the derived 3DP-NC framework, and corresponding SEM images of (b) 3DP-Zn-MOF and (c) 3DP-NC. (d) Schematic of the fabrication of the full cell using 3DP electrodes. Reproduced with permission [36]. Copyright 2019, Elsevier. (e) Schematic diagram of the fabrication process of the 3D-printed rGO/CNT microlattice, and (f) various layers (2–24 layers) to show the artificial adjustable thickness. Reproduced with permission [37]. Copyright 2020, Royal Society of Chemistry.

### 3.3. Three-Dimensionally Printed Electrolyte

Solid-state batteries generally maintain ideal inherent safety and stability, but the solid electrolytes used in these batteries usually have nonnegligible resistance. Solid-state lithium conductors such as garnet-type Li<sub>7</sub>La<sub>3</sub>Zr<sub>2</sub>O<sub>12</sub> (LLZ) have attracted significant attention. They are non-flammable materials, contrasting the volatile carbonate solvents and active lithium salts used in traditional lithium-ion battery electrolytes, which are regarded as the main cause of fire in these batteries, making these electrolytes a severe threat to the safety of the battery. In addition, solid electrolytes could also avoid the generation of metal dendrite during cycling process. Nevertheless, solid electrolytes still suffer from excessive battery impedance owing to the high resistance of the solid electrolyte itself and the high interface

impedance induced by insufficient electrode–electrolyte interfacial contact. Therefore, a new and novel designed electrolyte–electrode structure is crucial for the development of solid electrolytes. Recently, Hu et al. established multiple solid electrolyte inks with LLZ garnet as the model material through a 3D printing technique (Figure 4a) [38]. These inks maintain a wide range of rheological properties that are adjusted by changing the specific composition. The width of the printed product is influenced by the size of the nozzle, while the height of the features could be enhanced through adding additional layers. Figure 4b shows the schematic image of Li-filled pores between 3D-printed LLZ grids in a stacked-array pattern on an LLZ substrate. Based on the symmetric DC cycling of the cell at various current densities ranging from 0.1 to  $0.33 \text{ mA cm}^{-2}$ , there is a constant area-specific resistance, signifying the satisfactory conductivity. Three-dimensional electrolyte–electrode structures have several advantages over 2D planar electrodes, including higher areal loading capacity, faster ion diffusion, and lower tortuosity. The 3D printing process is regarded as a promising method for developing advanced batteries with complicated microstructures and appealing performance. Although great advances have been made in recent years, the shortcomings are still obvious. In previous works, post-processing steps such as heat treatment or freeze-drying are required to remove the solvent and template. When an even lower amount of the solvent is left, a severe distortion of the 3D structure might happen and significantly hinder its further application. Thus, Reza and coworkers successfully designed a high-temperature 3D printing technique and corresponding hybrid solid-electrolyte ink, which consisted of a solid polymer matrix and ionic-liquid electrolyte [39]. The solid polymer matrix could not only enhance the lithium diffusion rate but also increase the mechanical strength of the ink (Figure 4c). In addition, its viscosity and contact angles could also be precisely modified by the accumulation of white  $\text{TiO}_2$  particles (Figure 4d) [39]. Without any substrate surface treatment and electrolyte postprocessing, the hybrid electrolyte ink could be directly printed on the electrode, improving the efficiency of electrolyte preparation and further battery fabrication. During the printing process, the elevated temperature induced the formation of a unique dense electrolyte/electrode interface. As exhibited in Figure 4e, a full cell with a 3D Hilbert curved structure was printed, and the practical full cell battery composed of the printed hybrid electrolyte was finally assembled; the proof-of-concept was sealed with PDMS gel, demonstrating that the battery is printable in any shape, implying the great potential to implement this technique for power sources in energy storage devices with complex circuits. It can be concluded that the use of printed electrolytes in batteries generally leads to higher charge/discharge capacity and better rate performance compared to traditional solution-casting methods.

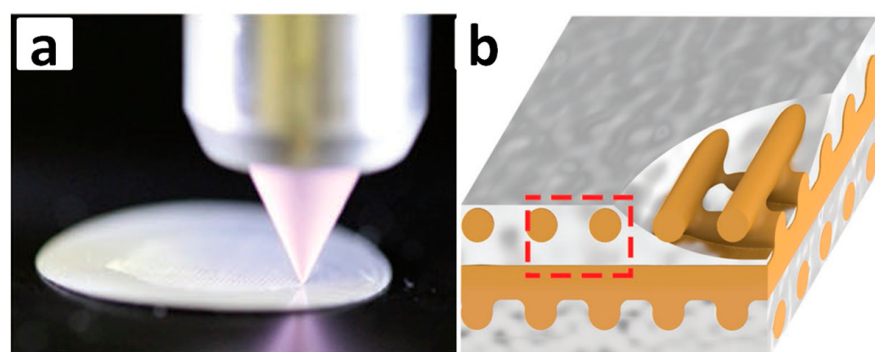


**Figure 4.** *Cont.*

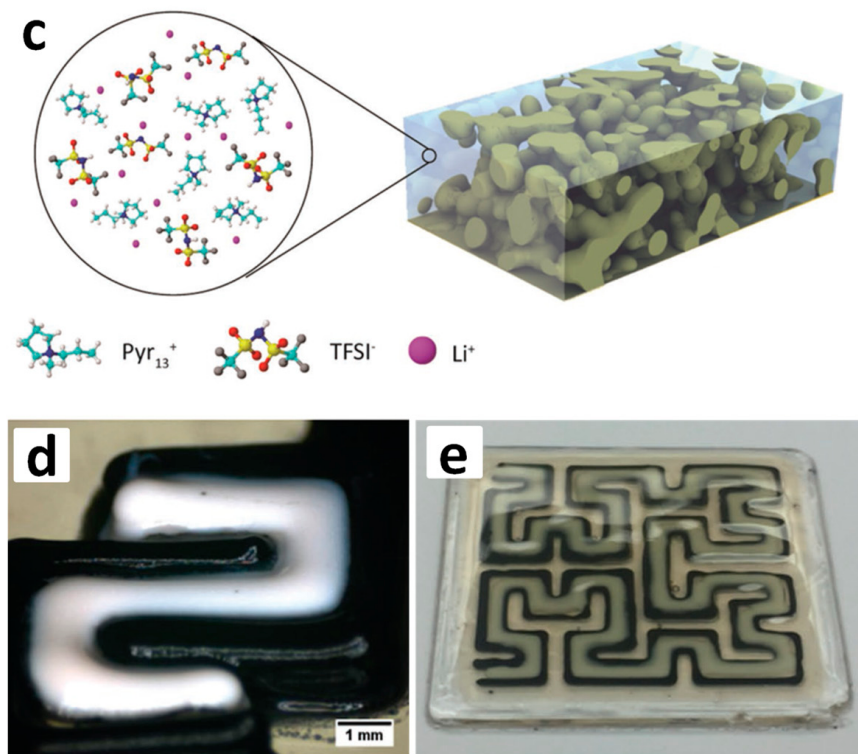


**Figure 4.** (a) Schematic of the process to 3D print solid electrolyte structures, and (b) schematic of Li-filled pores between 3D-printed LLZ grids in a stacked-array pattern on an LLZ substrate. Reproduced with permission [38]. Copyright 2018, Wiley. (c) Schematic image showing the microstructure of the PVDF-co-HFP/Pyr<sub>13</sub>TFSI/LiTFSI/TiO<sub>2</sub> hybrid solid-state electrolyte ink. Optical image of the 3D-printed (d) interdigitated full cell and (e) Hilbert curved structure full cell battery composed of LTO/INK-2/LFP. Reproduced with permission [39]. Copyright 2018, Wiley.

### 3.4. Three-Dimensionally Printed Membrane

When lithium makes contact with the electrolyte during the battery cycling process, there are often irreversible side reactions, such as “dead” lithium production, and even lithium dendrite construction, all of which pose serious safety risks. Aiming to overcome this bottleneck, massive efforts have been exerted to mitigate lithium nucleation and suppress the uncontrolled growth. Hu’s group proposed a thermal management separator by combining thermally conductive BN with the 3D extrusion process (Figure 5a), owing to its impressive stability, electrical insulation and outstanding mechanical strength [40]. Additionally, this separator has the potential to be applied to several additional battery chemistries, including sodium-ion, lithium-sulfur, and lithium-oxygen. In order to demonstrate the printing process, the circle spiral model has been used to produce a circular separator with a radius of 1.25 cm (Figure 5a). As illustrated in Figure 5b, under the set spacing, the adjacent spiral lines become connected with each other to form a helical and integrated film. Before being punched out into a disk with a radius of 8 mm and applied in the cell, the printed BN separator should be thoroughly vacuum-dried for 12 h. It is apparent that the dry BN separator can easily recover to its original shape after repeated folding, showing reliable flexibility (Figure 5c). In addition, it is shown that the Li symmetric cells including the BN separator exhibit enhanced voltage stability and reduced overpotential compared to the control separator for a cycling period exceeding 500 h.

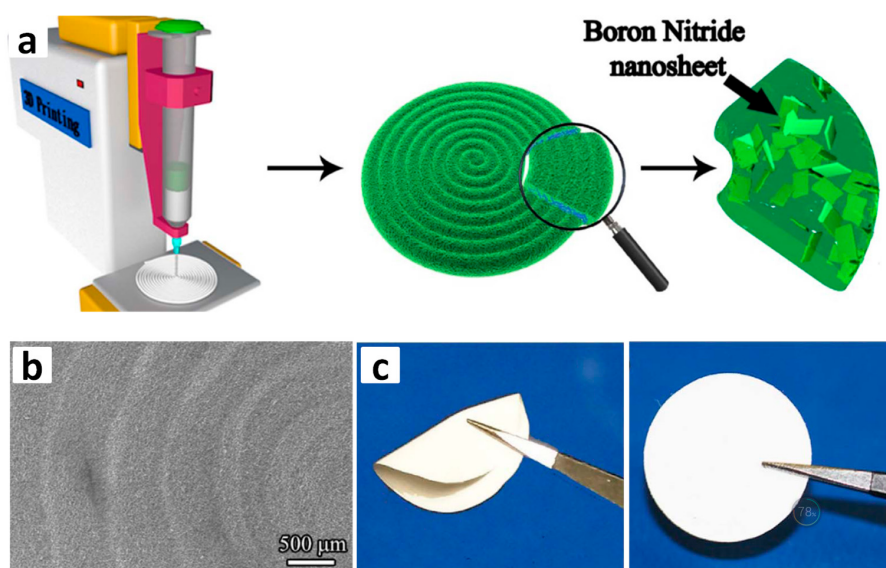


**Figure 5.** (a) Schematic illustration of the 3D printing apparatus, the BN in PVDF-HFP separator and the corresponding composition and structure. (b) SEM images for the top surface of the BN separator, and (c) twisted and recuperated BN separator. Reproduced with permission [40]. Copyright 2017, Elsevier.

To sum up, under controlled preparation conditions (e.g., temperature and humidity), battery components, such as the cathode, anode, electrolyte and membrane, with a rationally designed composition and structures can be successfully produced [41]. In addition, during battery performance characterization, the printed targeted components provide improved electrochemical properties. Three-dimensional printing technology can be leveraged to create energy storage components with tailored shapes and structures, enhancing the energy density, cycle stability and safety of the energy-related device (Table S2) [30,31,36,37,42–46]. In future research, it is expected that optimizing printing parameters, processes and target structures will become a crucial focus in the development of high-energy-density and stable printed materials.

#### 4. Supercapacitors

Three-dimensional printing technology has gradually become an important industrial technology due to its good flexibility in product designation and preparation. Notably, it has important applications and broad development space in several fields such as automobile manufacturing, implantable devices and new energy development.

Nevertheless, there is a dearth of comprehensive understanding among researchers about the intricacies of 3D printing technology. Furthermore, their attention tends to be narrowly directed towards print design, thereby impeding the realization of the versatile integration and application of 3D printing technology in conjunction with functional devices. With the flourishing of the new energy industry, new energy devices combined with 3D printing have emerged as a prominent research area. Yang et al. fabricated quasi-solid-state asymmetric micro-supercapacitors [47]. First, due to their high pseudocapacitance and desirable operating potential, graphene-vanadium nitride quantum dots (G-VNQDs) were printed on the surface of glass as the anode active material. Then, V<sub>2</sub>O<sub>5</sub> with high Faradic activity and natural abundance was 3D printed as a cathode material. Finally, the gel-like electrolyte was 3D printed into the channels between the anode and cathode, serving as a separator (Figure 6a), which was followed by thorough vacuum freeze-drying. Based on the lateral view and cross-sectional view of the 3D-printed VO<sub>x</sub>/rGO electrode (Figure 6b), the printed filaments exhibited good continuity and were tightly packed in layers, and its average thickness was around 100 μm. Additionally, the printed filaments were seamlessly bonded together without any significant collapse. (Figure 6c). The favorable interaction between the neighboring filaments could contribute to the enhanced structural stability

of the printed ultrathick electrodes. Furthermore, the abundant open macropores, developed as a consequence of solvent removal during freeze-drying, were highly beneficial for electrolyte penetration. Consequently, the micro-supercapacitor with a large areal mass loading of  $3.1 \text{ mg cm}^{-2}$  exhibited a wide electrochemical potential window of  $1.6 \text{ V}$  and an ultrahigh areal capacitance of  $207.9 \text{ mF cm}^{-2}$ . Additionally, a high areal energy density of  $73.9 \mu\text{Wh cm}^{-2}$  was also achieved, and the asymmetric supercapacitor showed good performance with a capacitance retention of 58.3% when the current density was increased from  $0.63$  to  $4.71 \text{ mA cm}^{-2}$  (Figure 6d). This reveals that the 3D printing strategy is efficient for use in the construction of various asymmetric micro-supercapacitors as energy storage systems. Additionally, Barg and coworkers first created 3D-printable inks using few-layered MXene flakes immersed in water, free from any additional sacrificial additives, and applied the inks to symmetric supercapacitors [48]. As shown in Figure 6e, wet 3D structures were subjected to freeze-drying in order to produce freestanding  $\text{Ti}_3\text{C}_2\text{T}_x$  structures with the structure ideally preserved and a low level of shrinkage; the individual printed filaments had a diameter of  $326 \pm 13 \mu\text{m}$ , achieving an interlaced architecture without bending (Figure 6f). This demonstrated that the viscoelastic properties of  $\text{Ti}_3\text{C}_2\text{T}_x$  inks are highly appropriate for the 3D printing of freestanding architectures. Aiming to illustrate the promise of MXene inks for the creation of energy storage devices,  $\text{Ti}_3\text{C}_2\text{T}_x$  electrodes were 3D-printed with tunable thickness and gaps (Figure 6g). Notably, this 3D-printed device achieved a high areal capacitance of  $2.1 \text{ F cm}^{-2}$  at  $1.7 \text{ mA cm}^{-2}$  and a gravimetric capacitance of  $242.5 \text{ F g}^{-1}$  at  $0.2 \text{ A g}^{-1}$  with a high retention (above 90%) after 10,000 cycles. It is expected that the proposed sustainable printing and design methodologies can be employed to create high-performance, multiscale and multidimensional functional structures for various applications. The outcomes validate the benefits of creating high-performance supercapacitors through 3D printing techniques which can promote the intricate design of electrodes and broaden the application range of supercapacitors. The advent of 3D printing technology has revolutionized the way we approach product design and fabrication. Researchers have demonstrated the successful fabrication of high-performance micro-supercapacitors using 3D printing strategies, achieving large areal capacitance, high energy density, and excellent electrochemical performance. These findings validate the potential of 3D printing techniques to create functional devices with intricate designs and broaden the application range of supercapacitors.

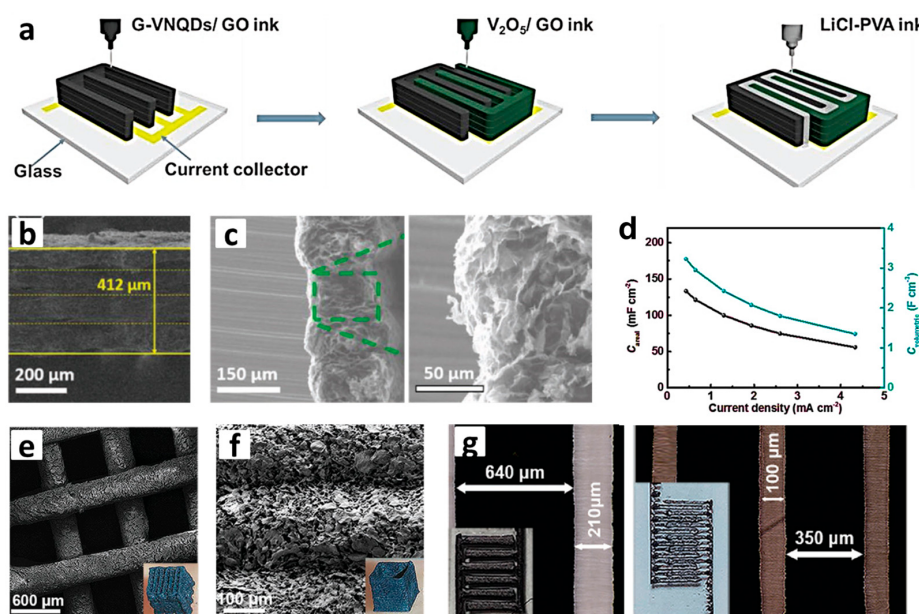


**Figure 6.** (a) Schematic illustration of 3D printing an asymmetric supercapacitor with interdigitated electrodes. SEM images of the (b) lateral view and (c) cross-sectional view of 3D-printed VO<sub>x</sub>/rGO

electrode. (d) Areal and volumetric capacitances of the 3D-printed  $\text{VO}_x/\text{rGO}/\text{G-VNQDs/rGO}$  asymmetric supercapacitor. Reproduced with permission [47]. Copyright 2018, Wiley. SEM and optical photographs (inset) of (e) a freestanding  $\text{Ti}_3\text{C}_2\text{T}_x$  microlattice and (f) hollow rectangular prism. (g) Optical microscopy images and optical photographs (inset) of 3D-printed interdigitated designs. Reproduced with permission [48]. Copyright 2019, Wiley.

## 5. Advanced Detection Techniques

Advanced detection techniques are essential for the realization of the comprehensive and meticulous analysis of 3D-printed samples. In Figure 7a–c, 3D topographic images of printed porous electrode with dual-gradient electron/ion fluxes are obtained through establishing a 3D gradient distribution of Ag nanoparticles (Ag NPs). Acute and unambiguous bumps dispersed on the surface of 3D-printed Zn electrode, and the up-bottom and homogeneous anodes show tendentious Zn dendrite. After implementing the gradient ion/electron flux mode, Zn metal tends to accumulate on the bottom layer, and no unusual protrusions are observed on the top surface, and the bottom-up structured anode maintains a minimal surface fluctuation [49]. The bottom-up attenuating distribution of conductive Ag NPs creates a bottom-aggregated electron flux. Meanwhile, due to the high binding energy between Ag and Zn atoms, Ag NPs have desirable zincophilic properties. It is beneficial for Zn ions to move toward and aggregate at the bottom of the electrode, which creates a new ion flux gradient [49]. In addition, Zhang et al. characterized the surface of a 3D-printed Zn-deposited nitrogen host (3DP-NC@Zn) and non-printed electrode (Bulk-NC@Zn) using laser confocal microscopy (Figure 7d,e). In the proposed 3D topographic images, the large clusters and uneven surface on the Bulk-NC@Zn electrode imply the rough deposition of Zn (Figure 7d), whereas Zn nanosheets are evenly spread out on the surface of the 3DP-NC host without any abnormal local projection (Figure 7e) [50]. COMSOL Multiphysics is a piece of software used for the coupling of multi-physics and simulating various physical processes in science and engineering, including 3D printing. In Figure 7f,g, the ionic flux distributions of Bulk-NC and 3DP-NC are simulated through COMSOL Multiphysics. The intense ionic flow concentrates  $\text{Zn}^{2+}$  at the apex of the electrode–electrolyte interface in the bulk NC host, boosting the polarization and accelerating Zn deposition. By introducing 3D printing technology, the ionic field is redistributed. Rather than accumulating on the surface, the  $\text{Zn}^{2+}$  ions mainly accumulate within the multi-channel structure (Figure 7g). The maximum ionic flux exists on the walls of reservoirs, inducing a preferable homogeneous Zn deposition along the walls of the reservoirs, thus mitigating the Zn growth occurring on the outermost layer of a surface [50]. Furthermore, COMSOL Multiphysics could also be used to investigate the stress distribution of 3D-printed material. As shown in Figure 7h, the elastic polyacrylamide network provided a low (1–10 MPa) and uniform stress distribution. The 3D-printed porous polyacrylamide network seen in Figure 7i has a favorable stress distribution, which enables the gradual dispersion of internal stresses throughout the process of  $\text{Zn}^{2+}$  plating/stripping. Consequently, this leads to little deformation [51]. Thus, it could be concluded that COMSOL Multiphysics is an ideal analysis method in 3D printing technology. In situ Raman spectroscopy was employed to examine the structural changes in 3D-printed electrodes. As shown in Figure 7j, the intensity of the  $v_1$  peak increases during charging. The ionic deintercalation process results in the formation of Mn (IV) and the reduction in the bond length between Mn and O. Meanwhile, the  $v_2$  peak is also intensive owing to the increased percentage of Mn (IV) and the shrinkage of the Mn-O bond along the  $\text{dx}^2-\text{y}^2$  orbital [52]. Additionally, the  $\text{Zn}^{2+}$  deintercalation process demands a substantial amount of energy, resulting in an elevated Raman signal [52]. Thus, advanced detection techniques illustrate their vital importance in 3D printing characterization. They are effective tools to unveil the microstructure and features of the printed products and are a helpful way to provide essential guidance for further structure optimization [53].

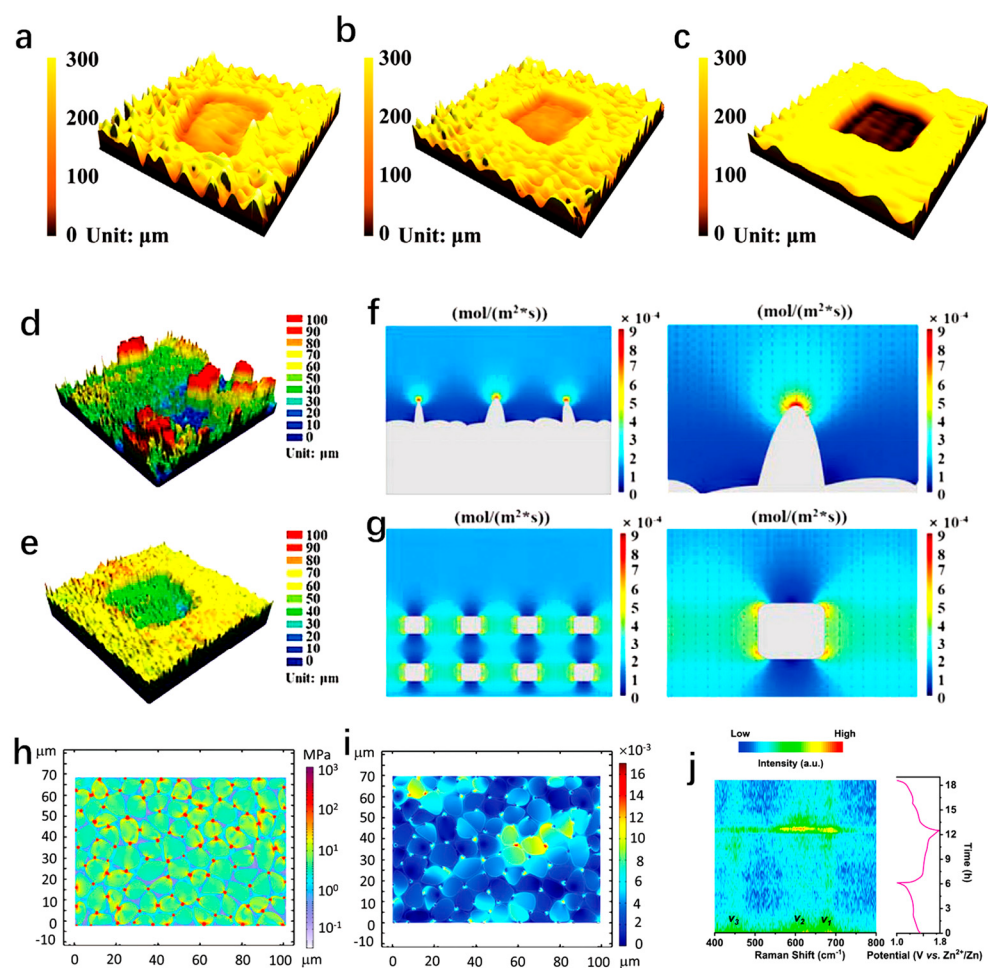


**Figure 7.** Three-dimensional topographic images of a 3D-printed Zn electrode with up-bottom (a), homogeneous (b) and bottom-up (c) attenuating Ag nanoparticles after cycling. Reproduced with permission [49]. Copyright 2018, Wiley. Laser confocal microscopy 3D topographic images of a (d) non-printed Zn-deposited bulk nitrogen-doped carbon host and a (e) Zn-deposited 3D-printed N-doped carbon host. Ionic flux distribution in (f) bulk-N-doped carbon and (g) 3D-printed N-doped carbon hosts simulated using COMSOL Multiphysics. Reproduced with permission [50]. Copyright 2018, Wiley. (h) Simulated stress distribution and (i) the deformation of the composite during  $\text{Zn}^{2+}$  plating/stripping. Reproduced with permission [51]. Copyright 2023, Wiley. (j) In situ Raman spectra of a 3D-printed  $\text{MnO}_2$  electrode during the discharging/charging process. Reproduced with permission [52]. Copyright 2018, Wiley.

## 6. Summary and Perspective

Three-dimensional printing, as a cutting-edge manufacturing and rapid prototyping technique, has been widely applied. One of the most fascinating application fields is electrical energy storage and conversion. In recent years, with the maturation of 3D printing technology, it has become quite easy to apply this technique to the development of energy storage and conversion devices. As a state-of-the-art technology, the additive manufacturing technique offers promising advantages in the field of electrode fabrication, and it has recently opened up new avenues for innovative industrial designs. In this review, the advances of 3D printing technology and recent research advances in electrocatalysis, secondary batteries, and supercapacitors are organized and summarized.

1. Three-dimensional printing can theoretically print any relatively complex structure. The application of the 3D printing technique has experienced a surge in popularity due to its advantages in terms of design flexibility, material efficiency, and the simplified creation of intricate structures. A diverse range of materials, including polymers,

metals, ceramics, thermosets, resins, and esters, may be further leveraged for 3D printing through various procedures.

2. With an increase in electrode thickness, the bulk structure experiences reduced ion diffusion rates due to the presence of an excessive amount of dead mass. This leads to a marked decrease in rate performance. Therefore, the advancement of multi-scale electrodes is particularly essential for attaining superior electrochemical performance. The application of 3D printing technology offers a potential solution for improving the performance of high-load electrodes. Versus conventional thick electrode fabrication techniques (coating and calendering), the 3D printing process can create 3D structured electrodes with shorter ion diffusion paths and lower resistance. Thus, higher energy density can be generated by creating porous structures with larger surface areas, improved electrode reactions and ions transport, and increased utilization of space.
3. Nowadays, there is a limited amount of research on applicable materials for 3D printing because this technology is still being refined and improved. Expanding the selection of materials for the 3D printing of electrochemical device components, as well as research and development on electrochemical energy-related applications, is still an important topic to be investigated.
4. Three-dimensional printing has clear technical advantages, but also limitations. It still cannot meet the requirements of large-scale production. Moreover, in some cases, the quality of 3D-printed products does not surpass traditional technologies, as completely controlling the void ratio, density and uniformity during printing process is still difficult. In addition, the materials available for 3D printing are still relatively limited, and the 3D-printed objects are easily affected by the external environment, such as temperature and humidity. To some extent, they hinder the wide application of 3D printing technology. It is essential to continuously optimize the production process to improve the quality and performance of energy storage devices.
5. The cost of 3D printing remains a significant challenge that needs to be addressed. Reduced 3D printing costs can drive the widespread adoption and application of this technology, allowing more people to benefit from its advantages. To reduce the cost, innovation, productivity and transformation in the manufacturing sector are highly needed. Simultaneously, adequate market competition, technological exchanges, and integration could also trigger effective cost reduction.

Overall, although obstacles still remain and additional effort is also needed, significant improvements have already been made in recent years. With the consistent and intentional exploration by researchers worldwide, advanced 3D printing technology could certainly change our lives with satisfactory electrical energy-related performance.

**Supplementary Materials:** The following supporting information can be downloaded at: <https://www.mdpi.com/article/10.3390/batteries9110546/s1>, Table S1: Brief summary of typical 3D-printed electrocatalysts; Table S2: Brief summary of typical 3D-printed battery electrodes.

**Author Contributions:** S.Z., Y.-J.Z. and G.Z. conceived and designed the structure of the review. Y.W. and P.L. collected the papers related to the topic of the review. S.Z. and S.X. wrote the manuscript. P.L., N.A. and G.Z. finished the language polishing. All authors have read and agreed to the published version of the manuscript.

**Funding:** This work was supported by Science Fund Program for Distinguished Young Scholars in Shandong (Overseas) (2023HWYQ-079), the Guangdong Basic and Applied Basic Research Program (Grant No. 2022A1515010649), and the Shenzhen Science and Technology Program (Grant Nos. JCYJ20210324095611032 and JCYJ20220818100008016).

**Conflicts of Interest:** The authors declare no conflict of interest.

## References

1. Steenhuis, H.-J.; Fang, X.; Ulusemre, T. Global Diffusion of Innovation during the Fourth Industrial Revolution: The Case of Additive Manufacturing or 3D Printing. *Int. J. Technol. Manag.* **2019**, *17*, 2050005.
2. Saadi, M.A.S.R.; Maguire, A.; Pottackal, N.T.; Thakur, M.S.H.; Ikram, M.M.; Hart, A.J.; Ajayan, P.M.; Rahman, M.M. Direct Ink Writing: A 3D Printing Technology for Diverse Materials. *Adv. Mater.* **2022**, *34*, 2108855. [[CrossRef](#)]
3. Bao, Y.; Paunović, N.; Leroux, J.-C. Challenges and Opportunities in 3D Printing of Biodegradable Medical Devices by Emerging Photopolymerization Techniques. *Adv. Funct. Mater.* **2022**, *32*, 2109864. [[CrossRef](#)]
4. Xu, L.; Thompson, C.V. Electrochemically controlled reversible formation of organized channel arrays in nanoscale-thick RuO<sub>2</sub> films: Implications for mechanically stable thin films and microfluidic devices. *ACS Appl. Nano Mater.* **2021**, *4*, 13700–13707. [[CrossRef](#)]
5. Ligon, S.C.; Liska, R.; Stampfl, J.; Gurr, M.; Mülhaupt, R. Polymers for 3D Printing and Customized Additive Manufacturing. *Chem. Rev.* **2017**, *117*, 10212–10290. [[CrossRef](#)]
6. Goh, G.L.; Zhang, H.; Chong, T.H.; Yeong, W.Y. 3D Printing of Multilayered and Multimaterial Electronics: A Review. *Adv. Electron. Mater.* **2021**, *7*, 2100445. [[CrossRef](#)]
7. Chen, Z.; Sun, X.; Shang, Y.; Xiong, K.; Xu, Z.; Guo, R.; Cai, S.; Zheng, C. Dense ceramics with complex shape fabricated by 3D printing: A review. *J. Adv. Ceram.* **2021**, *10*, 195–218. [[CrossRef](#)]
8. Costa, C.M.; Gonçalves, R.; Lanceros-Méndez, S. Recent advances and future challenges in printed batteries. *Energy Stor. Mater.* **2020**, *28*, 216–234. [[CrossRef](#)]
9. Yang, Y.; Yuan, W.; Zhang, X.; Yuan, Y.; Wang, C.; Ye, Y.; Huang, Y.; Qiu, Z.; Tang, Y. Overview on the applications of three-dimensional printing for rechargeable lithium-ion batteries. *Appl. Energy* **2020**, *257*, 114002. [[CrossRef](#)]
10. Liu, H.; Zhang, H.; Han, W.; Lin, H.; Li, R.; Zhu, J.; Huang, W. 3D Printed Flexible Strain Sensors: From Printing to Devices and Signals. *Adv. Mater.* **2021**, *33*, 2004782. [[CrossRef](#)]
11. Zhou, L.-Y.; Fu, J.; He, Y. A Review of 3D Printing Technologies for Soft Polymer Materials. *Adv. Funct. Mater.* **2020**, *30*, 2000187. [[CrossRef](#)]
12. Zeng, L.; Li, P.; Yao, Y.; Niu, B.; Niu, S.; Xu, B. Recent progresses of 3D printing technologies for structural energy storage devices. *Mater. Today Nano* **2020**, *12*, 100094. [[CrossRef](#)]
13. Gao, X.; Liu, K.; Su, C.; Zhang, W.; Dai, Y.; Parkin, I.P.; Carmalt, C.J.; He, G. From bibliometric analysis: 3D printing design strategies and battery applications with a focus on zinc-ion batteries. *SmartMat* **2023**, e1197. [[CrossRef](#)]
14. Shen, K.; Mei, H.; Li, B.; Ding, J.; Yang, S. 3D Printing Sulfur Copolymer-Graphene Architectures for Li-S Batteries. *Adv. Energy Mater.* **2018**, *8*, 1701527. [[CrossRef](#)]
15. Zhang, C.J.; Kremer, M.P.; Seral-Ascaso, A.; Park, S.-H.; McEvoy, N.; Anasori, B.; Gogotsi, Y.; Nicolosi, V. Stamping of Flexible, Coplanar Micro-Supercapacitors Using MXene Inks. *Adv. Funct. Mater.* **2018**, *28*, 1705506. [[CrossRef](#)]
16. Shi, H.H.; Pan, Y.; Xu, L.; Feng, X.; Wang, W.; Potluri, P.; Hu, L.; Hasan, T.; Huang, Y.Y.S. Sustainable electronic textiles towards scalable commercialization. *Nat. Mater.* **2023**. online ahead of print. [[CrossRef](#)]
17. Mubarak, S.; Dhamodharan, D.; Byun, H.-S. Recent advances in 3D printed electrode materials for electrochemical energy storage devices. *J. Energy Chem.* **2023**, *81*, 272–312. [[CrossRef](#)]
18. Zong, W.; Chui, N.; Tian, Z.; Li, Y.; Yang, C.; Rao, D.; Wang, W.; Huang, J.; Wang, J.; Lai, F.; et al. Ultrafine MoP Nanoparticle Splotched Nitrogen-Doped Carbon Nanosheets Enabling High-Performance 3D-Printed Potassium-Ion Hybrid Capacitors. *Adv. Sci.* **2021**, *8*, 2004142. [[CrossRef](#)] [[PubMed](#)]
19. Faria, R.; Marques, P.; Garcia, R.; Moura, P.; Freire, F.; Delgado, J.; de Almeida, A.T. Primary and secondary use of electric mobility batteries from a life cycle perspective. *J. Power Sources* **2014**, *262*, 169–177. [[CrossRef](#)]
20. Chia, H.N.; Wu, B.M. Recent advances in 3D printing of biomaterials. *J. Biol. Eng.* **2015**, *9*, 1–14. [[CrossRef](#)]
21. Gross, B.C.; Erkal, J.L.; Lockwood, S.Y.; Chen, C.; Spence, D.M. Evaluation of 3D printing and its potential impact on biotechnology and the chemical sciences. *Anal. Chem.* **2014**, *86*, 3240–3253. [[CrossRef](#)] [[PubMed](#)]
22. Peng, M.; Shi, D.; Sun, Y.; Cheng, J.; Zhao, B.; Xie, Y.; Zhang, J.; Guo, W.; Jia, Z.; Liang, Z. 3D Printed Mechanically Robust Graphene/CNT Electrodes for Highly Efficient Overall Water Splitting. *Adv. Mater.* **2020**, *32*, 1908201. [[CrossRef](#)] [[PubMed](#)]
23. Chang, S.; Huang, X.; Ong, C.Y.A.; Zhao, L.; Li, L.; Wang, X.; Ding, J. High loading accessible active sites via designable 3D-printed metal architecture towards promoting electrocatalytic performance. *J. Mater. Chem. A* **2019**, *7*, 18338–18347. [[CrossRef](#)]
24. Ying, Y.; Browne, M.P.; Pumera, M. Metal–organic-frameworks on 3D-printed electrodes: In situ electrochemical transformation towards the oxygen evolution reaction. *Sustain. Energy Fuels* **2020**, *4*, 3732–3738. [[CrossRef](#)]
25. Iffelsberger, C.; Ng, S.; Pumera, M. Catalyst coating of 3D printed structures via electrochemical deposition: Case of the transition metal chalcogenide MoS<sub>x</sub> for hydrogen evolution reaction. *Appl. Mater. Today* **2020**, *20*, 100654. [[CrossRef](#)]
26. Santos, P.L.D.; Rowley-Neale, S.J.; Ferrari, A.G.M.; Bonacin, J.A.; Banks, C.E. Ni-Fe (Oxy) hydroxide Modified Graphene Additive Manufactured (3D-Printed) Electrochemical Platforms as an Efficient Electrocatalyst for the Oxygen Evolution Reaction. *ChemElectroChem* **2019**, *6*, 5633–5641. [[CrossRef](#)]

27. Long, J.W.; Dunn, B.; Rolison, D.R.; White, H.S. Three-dimensional battery architectures. *Chem. Rev.* **2004**, *104*, 4463–4492. [[CrossRef](#)]
28. Chen, C.; Jiang, J.; He, W.; Lei, W.; Hao, Q.; Zhang, X. 3D Printed High-Loading Lithium-Sulfur Battery Toward Wearable Energy Storage. *Adv. Funct. Mater.* **2020**, *30*, 1909469. [[CrossRef](#)]
29. Li, J.; Leu, M.C.; Panat, R.; Park, J. A hybrid three-dimensionally structured electrode for lithium-ion batteries via 3D printing. *Mater. Des.* **2017**, *119*, 417–424. [[CrossRef](#)]
30. Wang, Y.; Chen, C.; Xie, H.; Gao, T.; Yao, Y.; Pastel, G.; Han, X.; Li, Y.; Zhao, J.; Fu, K. 3D-printed all-fiber li-ion battery toward wearable energy storage. *Adv. Funct. Mater.* **2017**, *27*, 1703140. [[CrossRef](#)]
31. Cai, J.; Fan, Z.; Jin, J.; Shi, Z.; Dou, S.; Sun, J.; Liu, Z. Expediting the electrochemical kinetics of 3D-printed sulfur cathodes for Li-S batteries with high rate capability and areal capacity. *Nano Energy* **2020**, *75*, 104970. [[CrossRef](#)]
32. Li, J.; Kong, Z.; Liu, X.; Zheng, B.; Fan, Q.H.; Garratt, E.; Schuelke, T.; Wang, K.; Xu, H.; Jin, H. Strategies to anode protection in lithium metal battery: A review. *InfoMat* **2021**, *3*, 1333–1363. [[CrossRef](#)]
33. Yuan, H.; Ding, X.; Liu, T.; Nai, J.; Wang, Y.; Liu, Y.; Liu, C.; Tao, X. A review of concepts and contributions in lithium metal anode development. *Mater. Today* **2022**, *53*, 173–196. [[CrossRef](#)]
34. Li, R.; Fan, Y.; Zhao, C.; Hu, A.; Zhou, B.; He, M.; Chen, J.; Yan, Z.; Pan, Y.; Long, J. Air-Stable Protective Layers for Lithium Anode Achieving Safe Lithium Metal Batteries. *Small Methods* **2023**, *7*, 2201177. [[CrossRef](#)] [[PubMed](#)]
35. Song, L.; Ning, D.; Chai, Y.; Ma, M.; Zhang, G.; Wang, A.; Su, H.; Hao, D.; Zhu, M.; Zhang, J.; et al. Correlating Solid Electrolyte Interphase Composition with Dendrite-Free and Long Life-Span Lithium Metal Batteries via Advanced Characterizations and Simulations. *Small Methods* **2023**, *7*, 2300168. [[CrossRef](#)]
36. Lyu, Z.; Lim, G.J.; Guo, R.; Pan, Z.; Zhang, X.; Zhang, H.; He, Z.; Adams, S.; Chen, W.; Ding, J. 3D-printed electrodes for lithium metal batteries with high areal capacity and high-rate capability. *Energy Stor. Mater.* **2020**, *24*, 336–342. [[CrossRef](#)]
37. Yan, J.; Zhi, G.; Kong, D.; Wang, H.; Xu, T.; Zang, J.; Shen, W.; Xu, J.; Shi, Y.; Dai, S. 3D printed rGO/CNT microlattice aerogel for a dendrite-free sodium metal anode. *J. Mater. Chem. A* **2020**, *8*, 19843–19854. [[CrossRef](#)]
38. McOwen, D.W.; Xu, S.; Gong, Y.; Wen, Y.; Godbey, G.L.; Gritton, J.E.; Hamann, T.R.; Dai, J.; Hitz, G.T.; Hu, L. 3D-printing electrolytes for solid-state batteries. *Adv. Mater.* **2018**, *30*, 1707132. [[CrossRef](#)] [[PubMed](#)]
39. Cheng, M.; Jiang, Y.; Yao, W.; Yuan, Y.; Deivanayagam, R.; Foroozan, T.; Huang, Z.; Song, B.; Rojaee, R.; Shokuhfar, T. Elevated-Temperature 3D Printing of Hybrid Solid-State Electrolyte for Li-Ion Batteries. *Adv. Mater.* **2018**, *30*, 1800615. [[CrossRef](#)]
40. Liu, Y.; Qiao, Y.; Zhang, Y.; Yang, Z.; Gao, T.; Kirsch, D.; Liu, B.; Song, J.; Yang, B.; Hu, L. 3D printed separator for the thermal management of high-performance Li metal anodes. *Energy Stor. Mater.* **2018**, *12*, 197–203. [[CrossRef](#)]
41. Shi, C.; Yu, M. Flexible solid-state lithium-sulfur batteries based on structural designs. *Energy Stor. Mater.* **2023**, *57*, 429–459. [[CrossRef](#)]
42. Foster, C.W.; Zou, G.Q.; Jiang, Y.; Down, M.P.; Liauw, C.M.; Ferrari, A.G.M.; Ji, X.; Smith, G.C.; Kelly, P.J.; Banks, C.E. Next-generation additive manufacturing: Tailorable graphene/polylactic (acid) filaments allow the fabrication of 3D printable porous anodes for utilisation within lithium-ion batteries. *Batter. Supercaps* **2019**, *2*, 448–453. [[CrossRef](#)]
43. Zhang, C.; Shen, K.; Li, B.; Li, S.; Yang, S. Continuously 3D printed quantum dot-based electrodes for lithium storage with ultrahigh capacities. *J. Mater. Chem. A* **2018**, *6*, 19960–19966. [[CrossRef](#)]
44. Saleh, M.S.; Li, J.; Park, J.; Panat, R. 3D printed hierarchically-porous microlattice electrode materials for exceptionally high specific capacity and areal capacity lithium ion batteries. *Addit. Manuf.* **2018**, *23*, 70–78. [[CrossRef](#)]
45. Airolidi, L.; Anselmi-Tamburini, U.; Vigani, B.; Rossi, S.; Mustarelli, P.; Quartarone, E. Additive Manufacturing of Aqueous-Processed  $\text{LiMn}_2\text{O}_4$  Thick Electrodes for High-Energy-Density Lithium-Ion Batteries. *Batter. Supercaps* **2020**, *3*, 1040–1050. [[CrossRef](#)]
46. Yee, D.W.; Citrin, M.A.; Taylor, Z.W.; Saccone, M.A.; Tovmasyan, V.L.; Greer, J.R. Hydrogel-Based Additive Manufacturing of Lithium Cobalt Oxide. *Adv. Mater. Technol.* **2021**, *6*, 2000791. [[CrossRef](#)]
47. Shen, K.; Ding, J.; Yang, S. 3D printing quasi-solid-state asymmetric micro-supercapacitors with ultrahigh areal energy density. *Adv. Energy Mater.* **2018**, *8*, 1800408. [[CrossRef](#)]
48. Yang, W.; Yang, J.; Byun, J.J.; Moissinac, F.P.; Xu, J.; Haigh, S.J.; Domingos, M.; Bissett, M.A.; Dryfe, R.A.; Barg, S. 3D Printing of Freestanding MXene Architectures for Current-Collector-Free Supercapacitors. *Adv. Mater.* **2019**, *31*, 1902725. [[CrossRef](#)] [[PubMed](#)]
49. He, H.; Zeng, L.; Luo, D.; He, J.; Li, X.; Guo, Z.; Zhang, C. 3D Printing of Electron/Ion-Flux Dual-Gradient Anodes for Dendrite-Free Zinc Batteries. *Adv. Mater.* **2023**, *35*, 2211498. [[CrossRef](#)]
50. Zeng, L.; He, H.; Chen, H.; Luo, D.; He, J.; Zhang, C. 3D Printing Architecting Reservoir-Integrated Anode for Dendrite-Free, Safe, and Durable Zn Batteries. *Adv. Energy Mater.* **2022**, *12*, 2103708. [[CrossRef](#)]
51. Shi, G.; Peng, X.; Zeng, J.; Zhong, L.; Sun, Y.; Yang, W.; Zhong, Y.L.; Zhu, Y.; Zou, R.; Admassie, S.; et al. A Liquid Metal Microdroplets Initialized Hemicellulose Composite for 3D Printing Anode Host in Zn-Ion Battery. *Adv. Mater.* **2023**, *35*, 2300109. [[CrossRef](#)] [[PubMed](#)]

52. Yang, H.; Wan, Y.; Sun, K.; Zhang, M.; Wang, C.; He, Z.; Li, Q.; Wang, N.; Zhang, Y.; Hu, H.; et al. Reconciling Mass Loading and Gravimetric Performance of MnO<sub>2</sub> Cathodes by 3D-Printed Carbon Structures for Zinc-Ion Batteries. *Adv. Funct. Mater.* **2023**, *33*, 2215076. [[CrossRef](#)]
53. Zhou, S.; Huang, S.; Yan, M.; Long, Y.; Liang, H.; Ruan, S.; Zeng, Y.; Cui, H.Z. A scalable, eco-friendly, and ultrafast solar steam generator fabricated using evolutional 3D printing. *J. Mater. Chem. A* **2021**, *9*, 9909–9917. [[CrossRef](#)]

**Disclaimer/Publisher's Note:** The statements, opinions and data contained in all publications are solely those of the individual author(s) and contributor(s) and not of MDPI and/or the editor(s). MDPI and/or the editor(s) disclaim responsibility for any injury to people or property resulting from any ideas, methods, instructions or products referred to in the content.